

# Invisible Base Electrode Coordinates Approximation for Simultaneous SPECT and EEG Data Visualization

L. Kowalczyk<sup>1</sup>, H. Goszczynska<sup>1</sup>, E. Zalewska<sup>1</sup>, A. Bajera<sup>2</sup>, L. Krolicki<sup>2</sup>

<sup>1</sup> Nałęcz Institute of Biocybernetics and Biomedical Engineering PAS, Department of Neuroengineering, Ks. Trojdena 4 str., 02-109 Warsaw, Poland

<sup>2</sup> Medical University of Warsaw, Department of Nuclear Medicine, Banacha 1a str., 02-097 Warsaw, Poland  
leszek.kowalczyk@hotmail.com, hgoszczynska@ibib.waw.pl

This work was performed as part of a larger research concerning the feasibility of improving the localization of epileptic foci, as compared to the standard SPECT examination, by applying the technique of EEG mapping. The presented study extends our previous work on the development of a method for superposition of SPECT images and EEG 3D maps when these two examinations are performed simultaneously. Due to the lack of anatomical data in SPECT images it is a much more difficult task than in the case of MRI/EEG study where electrodes are visible in morphological images. Using the appropriate dose of radioisotope we mark five base electrodes to make them visible in the SPECT image and then approximate the coordinates of the remaining electrodes using properties of the 10-20 electrode placement system and the proposed nine-ellipses model. This allows computing a sequence of 3D EEG maps spanning on all electrodes. It happens, however, that not all five base electrodes can be reliably identified in SPECT data. The aim of the current study was to develop a method for determining the coordinates of base electrode(s) missing in the SPECT image. The algorithm for coordinates approximation has been developed and was tested on data collected for three subjects with all visible electrodes. To increase the accuracy of the approximation we used head surface models. Freely available model from Oostenveld research based on data from SPM package and our own model based on data from our EEG/SPECT studies were used. For data collected in four cases with one electrode not visible we compared the invisible base electrode coordinates approximation for Oostenveld and our models. The results vary depending on the missing electrode placement, but application of the realistic head model significantly increases the accuracy of the approximation.

**Keywords:** EEG electrodes, SPECT, multimodal co-registration, EEG mapping, BioImage Suite, 3D image reconstruction.

## 1. INTRODUCTION

DEVELOPMENT of the neuroimaging techniques aims towards comprehensive evaluation of data collected in simultaneous morphological and functional examinations. Interpretation of the results requires adjustment of the images from both examinations in common coordinates. In advanced systems applied in MRI/EEG examinations the electrodes are visible in morphological images. This solution is not possible in simultaneously conducted SPECT and EEG studies. Lack of anatomical data in SPECT images is the issue to be addressed for the registration of EEG and SPECT data, especially in the case when hybrid SPECT-CT system is not available.

Comprehensive analysis of overlapped SPECT and EEG images might be helpful in, e.g., epileptic foci localization. Known methods [1, 2] give the accuracy of the focus location approximately equal to 80 % or, at times, it can be only determined with the accuracy to the left or right brain hemisphere.

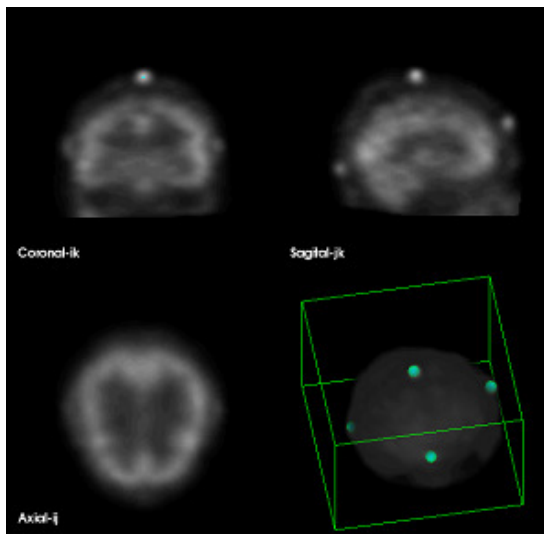
In our previous study we have developed a method for superposition of SPECT images and EEG maps implemented in our APW software when these two examinations are performed simultaneously [3]. This work was performed as part of a larger research concerning feasibility of improving the localization of epileptic foci, as compared to the standard SPECT examination, by applying the technique of EEG mapping. Developed method makes it possible, after further enhancements, to calculate the foci coordinates in SPECT scan space, to improve SPECT image

co-registrations in differential techniques [13], and to estimate particular brain region activity during simultaneous EEG/SPECT examination

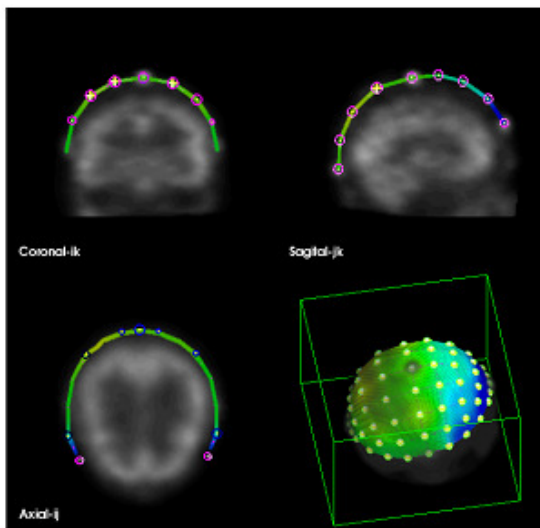
The method relies on making a few EEG electrodes (so-called base electrodes) visible in SPECT images using an appropriate dose of radioisotope [3, 4], calculating the coordinates of these electrodes in SPECT image space, approximating the coordinates of the remaining electrodes used in EEG recording and then computing a sequence of 3D EEG maps spanning on all electrodes (Fig.1.). SPECT examinations were performed using VARICAM SPECT system scintigraphic camera and SIEMENS SYNGO MI Work Station simultaneously with EEG recordings using Aura 24 system (Grass, USA). The procedure for marking base EEG electrodes to prevent the SPECT image quality degradation has been devised and tested by the authors in experiments with Jaszczak and Hoffman phantoms (<http://www.spect.com/products-all.html>) and in a pilot clinical study.

For the approximation of the coordinates of the base electrodes we have proposed a model of nine ellipses in 3D space determining the coordinates of all the electrodes of the enhanced 10-20 system of the EEG electrode placement [5]. The BioImage Suite software [6] has been applied for developing this method together with our own application for EEG and SPECT data processing. The BioImage Suite software is used especially for import of SPECT data with visible base electrodes and determination of base electrode coordinates. Approximation of the coordinates of the remaining electrodes of the 10-20 system and generation of

EEG 3D map in the space SPECT data have been performed using our own APW software design for EEG signal analysis.



a)



b)

Fig.1. Five EEG electrodes visible in SPECT images a) and 3D EEG map spanning on all the electrodes b).

Assuming the exact placement of the base electrodes the accuracy of the proposed method is assessed to be within the range of 5.5 mm. This is very close to the other methods [7, 8] which claim comparative accuracy of up to 5 mm. To increase the accuracy it would be justified to mark more than five electrodes. However, marking more electrodes could highly increase the risk of over saturating SPECT images, and thus, reducing the quality of the examination or even corrupting the results completely.

The advantage of the proposed method is the lack of requirement for any additional equipment. Besides easier introduction it does not increase the examination time significantly, it eliminates the sources of possible errors caused by the measuring procedures (electromagnetic, ultrasound) preceding SPECT examinations and possible

errors related to coordinates transformation from the measurement devices to SPECT image space.

Unfortunately, this is not always the case that the method of EEG map visualization on SPECT images acquired during simultaneously performed examinations provides the expected results. Out of 11 examinations we have performed, only in three of them all five base electrodes were clearly visible and in four cases four electrodes were visible. In the remaining examinations the number of invisible electrodes was two (in three cases) and in one case the visibility of the electrodes was so bad that only two out of five electrodes were visible in SPECT images.

Our experience indicates that this depends mainly on the procedure accuracy of radioisotope placement. Besides that, SPECT images are normalized to maximize the range of visualized intensities. Thus, the radioactive component placed under the electrode may be relatively high or relatively low.

In cases when not all electrodes are visible it is important to have a method for approximation of the coordinates of these missing electrodes to allow the application of the mapping procedure.

The aim of the current study was to develop a method for determining the coordinates of the base electrodes missing in the SPECT image.

## 2. SUBJECT AND METHODS

The method of EEG-SPECT data alignment described in [3] assumes that five electrodes (Cz, Oz, Fpz, T3, T4), so-called base electrodes, are visible in SPECT images. The algorithm of invisible base electrode approximation (IBEA) has been developed to approximate the coordinates of invisible base electrodes and, therefore, to enable superposition of SPECT images and EEG maps in case of incomplete data, i.e., not all base electrodes visible in SPECT images. This procedure uses our nine-ellipses model, also used for interpolation of EEG maps (Fig.2.) [3].

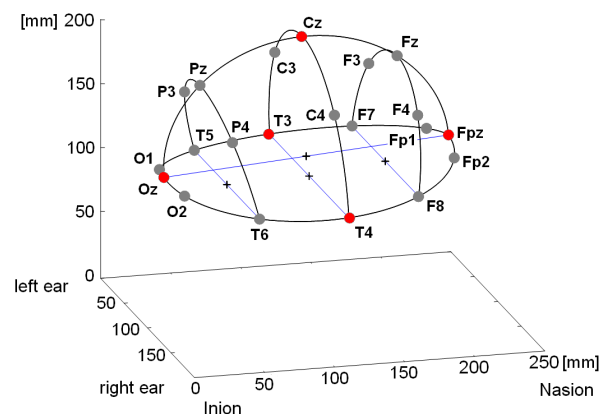


Fig.2. Nine-ellipses model of 10-20 electrodes placement system with marked base electrodes.

Below, the main assumptions of IBEA algorithm are presented.

*A. IBEA algorithm assumptions*

The coordinates of the invisible electrode can be approximated purely depending on the geometrical relationships between positions of electrodes of the 10-20 system. In the next step we will use SPECT data to achieve better accuracy of the approximation.

IBEA algorithm assumptions are as follows:

1. Electrodes placed according to the 10-20 system are placed on the head surface according to well defined rules [5] and are located closely to the theoretical positions defined by our nine-ellipses model, as described previously [3].
2. Electrode placement is highly repeatable when performed in the same laboratory as the same personnel uses the same equipment and follows the 10-20 system.
3. From the above assumptions we can approximate certain geometrical properties of the electrode coordinates which are usually met, with good accuracy (for example ratios between certain distances should be nearly constant).
4. Possible electrode locations are limited to the surface of the head, so they cannot be placed in the areas of SPECT 3D images of high intensity, as these areas indicate the interior of the skull. The head surface can be roughly approximated from SPECT images.

*B. Electrode placement models*

The assumption 2 mandates the creation and use of a statistical model of five base electrode placements specific for the particular laboratory. As a reference model we used the publicly available electrode placement model based on common head model computed by Oostenveld [9,10] named here Model Oost.

We have also developed our own model which is based on our EEG/SPECT data of five examinations with five or four electrodes visible, named Model Lab.

Model Lab calculations required initial alignment of the head layout in SPECT examination as corrections of line indicated by occipital and forehead electrodes position and vertex electrode position. Then the average electrode locations are interpolated according to the data from several examinations.

*C. Modes of electrode coordinates approximation*

Three ways of the approximate electrode coordinates calculation are described below. The calculations depend on the position of the missing electrode and can be divided into three modes:

- a. Approximation of coordinates of electrodes **Fpz** or **Oz**,
- b. Approximation of coordinates of electrodes **T3** or **T4**,
- c. Approximation of coordinates of electrode **Cz**.

*C.a. Electrode Fpz or Oz*

For these two electrodes we proposed two distinct methods – model based method and geometric method.

*Model based method*

This algorithm uses the data of the selected model of electrode placement and is based on the following assumptions:

1. Electrodes **Fpz** and **Oz** are located on the head symmetry axis.
2. From the properties of the 10-20 system the middle of a section defined by electrodes **Fpz** and **Oz** is very close to the plane defined by electrodes **Cz**, **T3** and **T4**. Here, we need to assume it is located precisely on the plane as no better approximation is available with so few electrodes.
3. Let us introduce the following symbols:
  - a. **SG** – head center, which is the middle of the section defined by electrodes **Fpz** and **Oz**
  - b. **SE2** – the middle of the section defined by electrodes **T3** and **T4**
4. We can compute a reference ratio (in the selected model space) between the following distances  $R1 = |Cz, SG| / |Cz, SE2|$ .
5. We can then compute the coordinates of **SE2** in the space of the examination and using the ratio **R1** approximate the coordinates of **SG** in the space of the examination.
6. Once the coordinates of **SG** are known the coordinates of electrode **Fpz** or **Oz** can be quickly found. The algorithm is symmetric and nearly the same calculations are used for **Fpz** and **Oz** coordinates approximation.

The above solution may yield precise results, if the head shape is very similar to the shape described by the selected model. But we found that the ratio of **SG** and **SE2** may be variable in a wide range, depending on subtle changes of electrode **T3** and **T4** locations, thus, producing large error of **Fpz** or **Oz** electrode coordinates approximation. The induced error of coordinates of **Oz** or **Fpz** may be two times greater than the error in localization of **SG**.

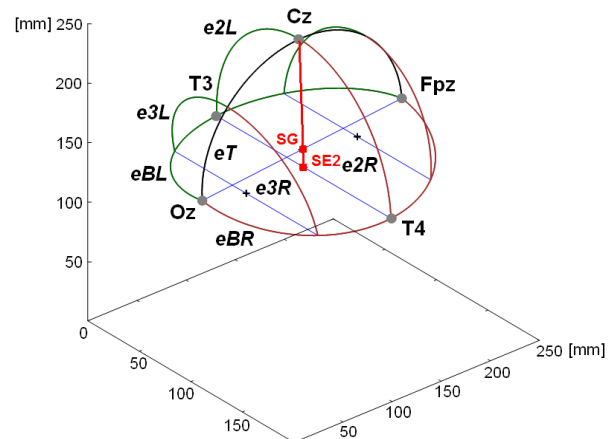


Fig.3. Algorithm 1 for Fz and Oz approximation. The ratio between the known sections Cz-SG and Cz-SE2 allows determination of the position of electrodes Fz or Oz.

*Geometric method*

Another approach for the approximation of electrodes **Fpz** and **Oz** was proposed, based only on one assumption described below and on the 10-20 system properties:

Section **|Fpz, Oz|** is perpendicular to the plane defined by three electrodes **T3, Cz** and **T4**.

This means that **Oz** (or **Fpz**, respectively) can have its coordinates mirrored from the existing electrode **Fpz** (or **Oz**), relative to the plane defined by electrodes **T3, Cz, T4**.

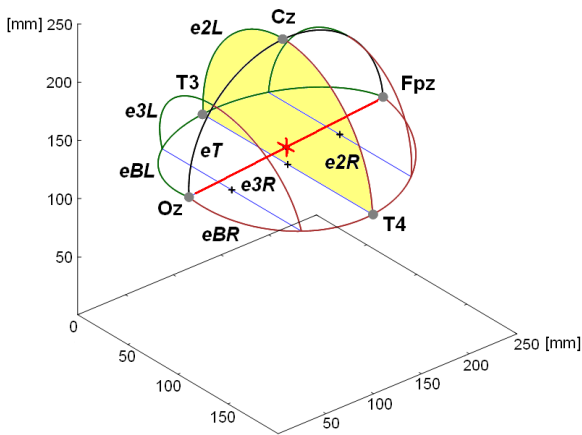


Fig.4. Algorithm 2 for Fz and Oz approximation. Mirroring the electrode Fpz or Oz against (plane T3, C3, T4) allows determination of electrode Oz or Fpz coordinates (respectively).

*C.b. Electrodes T3 or T4*

Electrodes T3 and T4 are placed symmetrically on the head surface. If one of them is invisible then it is enough to mirror the visible one against the plane defined by electrodes **Fpz, Cz** and **Oz**. The accuracy of this method depends entirely on the accuracy of the electrode placement on the head surface and on the head symmetry.

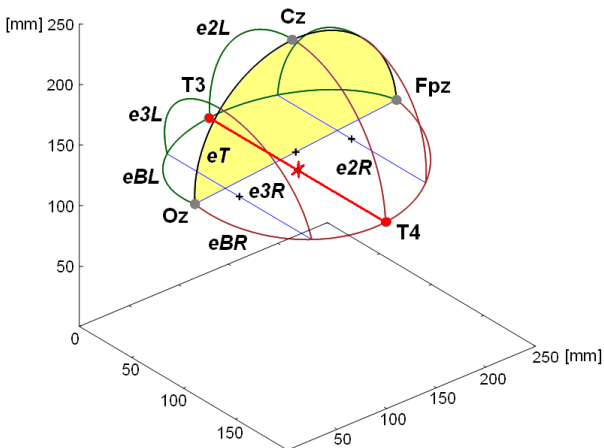


Fig.5. Algorithm for T3 and T4 approximation. Mirroring the electrode T3 or T4 against plane (Fpz, Cz, Oz) allows determination of electrodes T4 and T3 coordinates (respectively).

*C.c. Electrode Cz*

The algorithm is based on the geometrical properties of the 10-20 system and also on the properties of the selected model. We assume that the plane parallel to sections **Fpz-Oz** and **T3-T4** is perpendicular to the section **Cz-SG** (where **SG** is the middle of the section **Fpz-Oz**). We can compute the ratio **R2** (1) of the following distances in the model space.

$$R2 = |Fpz, Oz| / |Cz, SG| \tag{1}$$

As we know the coordinates of **Fpz, Oz** and **SG**, and as the section **Cz-SG** is perpendicular to the plane defined by **Fpz-Oz** and **T3-T4**, we can easily compute **Cz** coordinates utilizing the ratio **R2** calculated earlier.

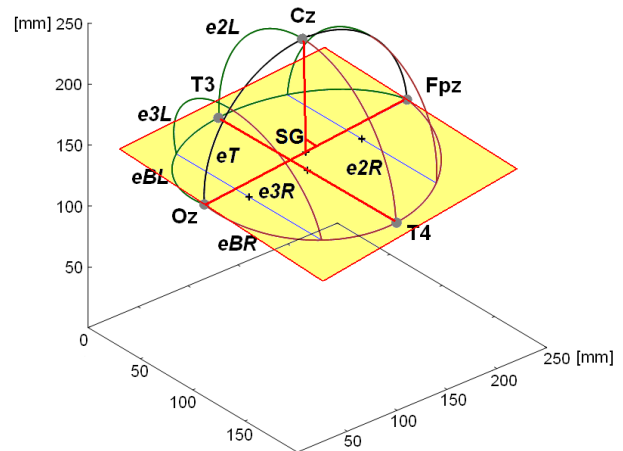


Fig.6. Algorithm for Cz approximation. Section Cz-SG is perpendicular to the plane defined by sections Fpz-Oz and T3-T4. The ratio between the length of section Fpz-Oz and Cz-SG is calculated according to the selected head model.

Alternative approach similar to the earlier described Algorithm 1 for electrodes **Fpz** and **Oz** approximation (so utilizing ratios between certain distances in the analyzed examination) proved to be very inaccurate for electrode **Cz** approximation.

*D. Corrections of approximated coordinates*

The simple calculations described above do not impose any reasonable limits to approximated coordinates of the electrodes. Thus, the electrode may be placed inside the head or far away from the head surface, as defined by corresponding SPECT examination, which is obviously wrong.

To compensate for this problem we apply certain corrections in the second step of the approximation process. It is based on a search for the head surface (as defined by certain value of SPECT data voxels). We search for certain threshold voxel value along the line **L** between the approximated electrode and the head center (**SG** - as defined earlier) and define it as a point on the approximated head surface. To compensate for the size of the electrodes, once we have the surface of the head located, we move the

electrode away from the head (along the line **L**) by half of the electrode diameter.

As the above procedure can accurately place the electrodes on the head surface, the crucial element for the whole algorithm accuracy is finding the appropriate 3D angle between the head axis and the approximated position of the electrode. If the angle is wrong (so the first step of the approximation produces high error) the described procedure will only place the searched electrode on the head surface, thus, making the coordinate of the electrode physically correct, but it will not significantly improve its position relative to the real localization of the electrode.

### 3. RESULTS

In section *A* below we present the procedure of preliminary data analysis for validation of our algorithms. The algorithm for coordinates approximation has been tested on data collected for subjects with all visible based electrodes (section *B*). For subjects with 4 visible electrodes we compare the invisible base electrode coordinates approximation for Oost model and for our Lab models (section *C*).

#### A. Base electrode visibility on SPECT images

The procedure of statement of invisibility of base electrode was preliminarily visually performed in sequences of three reconstructed projections of SPECT images for each person (Fig.7.).

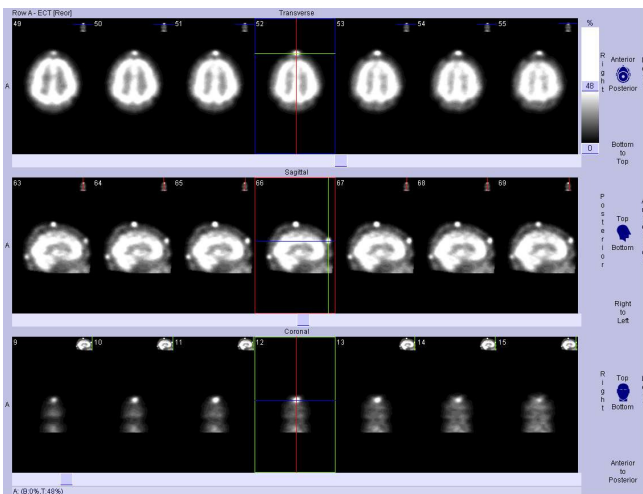


Fig.7. Example of three reconstructed SPECT projections (from SIEMENS SYNGO MI Work Station) for Subject 4 with marked visible frontal electrode.

The preliminarily estimated coordinates of the visible base electrodes for 11 examinations are shown in Table 1. The coordinates are enumerated in the order of respective projections in Fig.7. (bottom to top, right to left, anterior to posterior, comp. Fig.2. - bottom to top, right ear to left ear, inion to nasion) and are equal to the index of the middle frame with sequences with visible electrode. For the accurate coordinates calculations used for nine-ellipse model calculation the genuine SPECT images (Fig.8.) were analyzed in image processing software (Image Pro Plus and

BioImage Suite) using standard segmentation procedures as threshold operation.

Table 1. Coordinates (in voxel space, rounded to the nearer voxel) of the visible base electrodes for 11 examinations; symbol *x* denotes lack of data.

Sub. id	Electrodes				
	Fpz frontal	T4 right temporal	Oz occipital	T3 left temporal	Cz vertex
1	42, 65, 22	22,26, 96	46, 65, 121	x	X
2	66, 65, 44	x	x	x	74, 65, 77
3	72, 65, 42	x	x	37,102, 69	78, 65, 70
4	52,66, 12	40,23, 60	27, 66, 105	40,108, 60	78, 66, 63
5	50,65, 22	x	26, 62, 117	35,104, 75	74, 69, 76
6	x	39, 21, 68	44, 58, 118	36,104, 68	84, 72, 72
7	50, 62, 30	34, 27, 74	x	x	81, 71, 73
8	56, 65, 25	41,28, 71	35, 65, 118	41,104,64	83, 61, 81
9	51, 72, 29	37,26, 78	x	38,107,78	82, 67, 78
10	46, 57, 15	32,26, 68	49, 57, 109	34,105, 55	84, 67, 60
11	31, 61, 14	x	66, 58, 101	35,101, 58	80, 61, 47

The values of coordinates of base electrodes were obtained as center of mass and center of gravity of 3D objects reconstructed from sequences of genuine SPECT images as shown in Fig.8. The differences between these two kinds of measurements were less than 0.1 %.

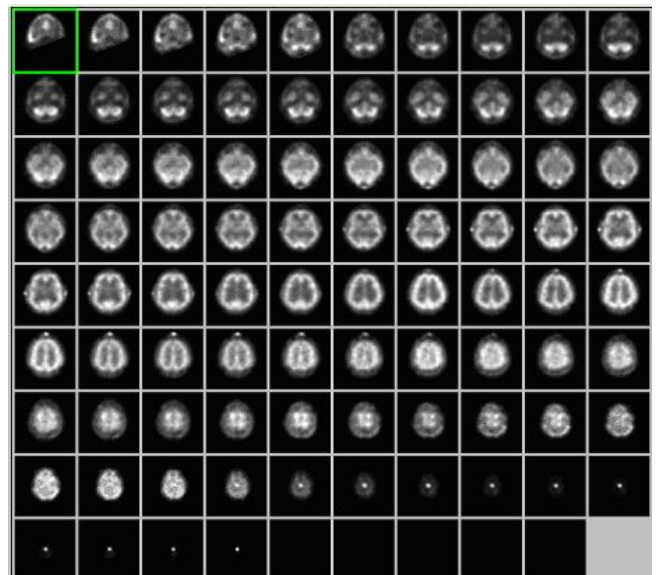


Fig.8. Sequences of genuine SPECT images for Subject 4.

The IBEA algorithm for coordinates approximation has been tested on data collected for three subjects with all visible electrodes.

*B. Estimation of method errors*

To assess the accuracy of the proposed approximation method we performed the calculations using the data from three examinations with all the base electrodes visible (subjects 4, 8, 10, Table 1., in red). We applied the IBEA algorithm to search for each base electrode coordinates using the coordinates of the remaining electrodes. Then we compared the coordinates from the examinations to these produced by the IBEA algorithm to get the average error of the proposed algorithm. The average error of the localization of the electrodes for all the approximation methods implemented was calculated: 14.5 mm, 17.4 mm and 29.9 mm, for three analyzed subjects, respectively. The significant error in the last case was mostly caused by a displacement (mishandling) of the base electrodes from the standard positions which invalidate many of the algorithm assumptions.

The errors in mm for the electrodes approximated according to the purely geometrical approach and using two models are provided in Table 2.

Table 2. Errors in [mm] for the electrodes approximated according to the purely geometrical approach and using two models.

Method	Subject 4	Subject 8	Subject 10
Geometric approximation	20.9	21.7	32.5
Approximation based on Model Oost	18.0	13.8	31.9
Approximation based on Model LAB	17.2	12.7	29.1

The comparison of the errors of electrode **Fpz** approximation using the geometric method and the model based method is presented in Table 3.

Table 3. Comparison of the errors of electrode Fpz approximation, in [mm].

Method	Subject 4	Subject 8	Subject 10
Geometric approximation	35.2	20.4	13.2
Approximation based on Model Oost	19.3	13.7	34.0
Approximation based on Model LAB	20.1	13.6	33.4

The improvement of electrode coordinates approximation with the use of SPECT data comparing to plain geometric and model based approach for electrodes **Cz** and **Oz** (in [mm]) is presented in Table 4.

Table 4. Approximation improvement from the use of SPECT data (in mm and relative to the total approximation error).

Electrode	Subject 4	Subject 8	Subject 10
Cz	3.1 (20 %)	0.6 (5%)	7.4 (27%)
Oz	2.6 (8%)	3.9 (19%)	5.9 (46%)

*C. Approximation of invisible electrode coordinates*

For subjects with four visible electrodes (blue in Table 1.) we compared the invisible base electrode coordinates approximation for all proposed algorithms, for the Oost model, and for our models. Examples of visualization of location of missing electrodes are presented in Fig.7.

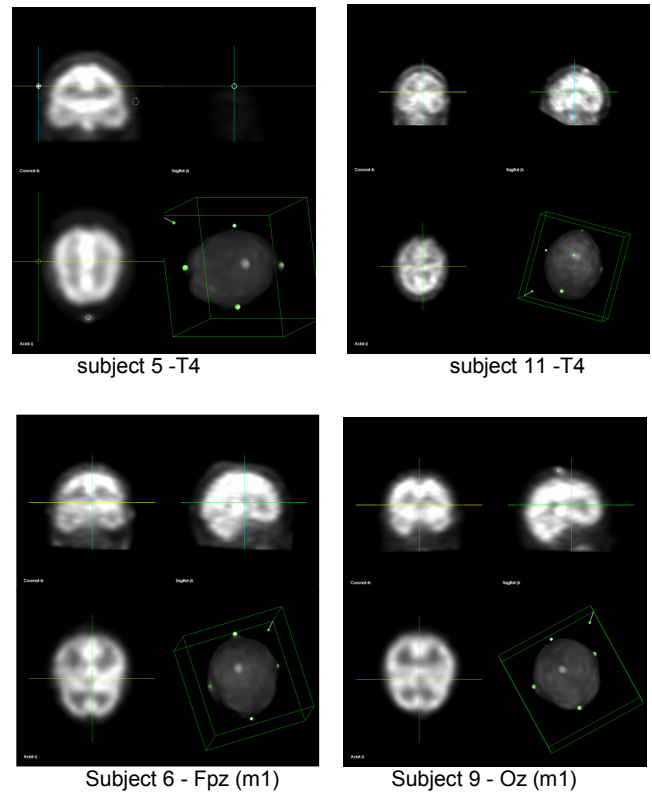


Fig.9. Locations of approximated electrodes for four subjects.

Table 5. presents the differences between positions of approximated electrodes for the proposed algorithms.

Table 5. Comparison of the location of electrode approximated electrodes in voxel space coordinate system (used in Fig.7.).

Subject id	Method	Fpz frontal	T4 right temporal	Oz occipital	T3 left temporal	Cz vertex
5			45, 21, 76			
6	model based: Oost LAB	45, 70, 16 45, 70, 17				
	geometric average	53, 58, 17 49, 64, 16				
9	model based: Oost LAB			36, 62, 118 36, 62, 118		
	geometric average			47, 72, 116 41, 67, 119		
11			44,17,52			

### 3. DISCUSSION

At present, the algorithm can only approximate the coordinates of one missing electrode, so four of five base electrodes must be clearly visible in SPECT images. The algorithm could not be easily extended to cope with the cases where two or more electrodes are invisible without significant accuracy loss as in most cases it uses the coordinates of all four electrodes to approximate the localization of the missing fifth electrode. If lower accuracy is allowed then similar calculations could be used to determine approximate localization of two invisible electrodes out of the set of five.

The main source of error of the presented algorithm results from the fact that the model used for calculations is not a representative for the group of subjects. The variability of the heads shapes (including their asymmetry) can be large and any approach utilizing one head model will be inaccurate in some cases.

Proper testing of the proposed algorithm for SPECT based adjustment of electrode coordinates faces certain difficulties. When we use examinations with all base electrodes visible, then the presence of the electrodes in SPECT images slightly spoils the results of SPECT based approximation, as we assume the electrode should lay on the head surface, while the surface is artificially elevated around the electrode visible in the SPECT examination. If we take an examination where the electrode is really not visible then it will not spoil SPECT based coordinates approximation, but we then do not have proper reference coordinates of the invisible electrode.

It is crucial to properly set the value of the voxels, which corresponds well with the imaginative head surface in SPECT examination. There are differences between examinations in the average level of voxel values and this must be compensated by proper adjustment of the algorithm parameters. Visual inspection of the results seems to be currently the best way to achieve good results, but it should also be possible to use histogram based analysis to estimate this parameter automatically. The largest value on the histogram should correspond to the background. The few voxel intensities next to the value of the background are the candidates for the probable head surface.

The errors (for model based approximation) for some electrodes seem to be consistent, and thus, a modification of the algorithm could be proposed where additional corrections could be applied. For each electrode the model would have a 3D correction vector defined that is applied after the basic calculations are finished, but before the adjustment to head surface is computed (based on SPECT data). However, for such a small data set we did not attempt to implement such enhancement.

The errors of localization of the electrodes are smaller by 1-2 mm when Model LAB is used, as compared to Model Oost (Table 2.). We expect that further refinements of the LAB model could provide even better approximation results. It justifies the use of custom models, built according to the data from examinations performed by the same laboratory. We computed our model from only five

examinations (subjects 4, 8, 10, 5 and 11). To establish a reliable model, at least ten times more examinations would have to be considered.

For electrodes **Fpz** (and **Oz**, as the approximation is calculated in the same way) the results of both algorithms are comparable (Table 3.), though both produce inaccurate results in our tests (the error may exceed 3 cm). It might be reasonable to use the average result of both algorithms, as for the few examinations we checked they produce results shifted in the opposite directions from the correct coordinates. Unfortunately, we do not have enough data to justify such approach and to provide a convincing reason for such opposite shifting of the results.

More tests would have to be performed, and the use of a better LAB model could improve the results of model based approximations.

Adjustment of the approximated coordinates to the head surface is a good enhancement of the procedure as indicated by the results presented in Table 4.

The individual anatomical head differences were assessed to be in the range of 20 mm [12].

There is also another potential application of the presented method in elaborated study concerning visible base electrode segmentation. Due to potential very low intensity of base electrode in SPECT image there could appear some ambiguity in proper indication and segmentation process of this base electrode. Algorithm of approximation of the coordinates of the missing electrode might support this process by additional information from model of electrode coordinates.

### 4. CONCLUSIONS

The algorithm IBEA – Invisible Base Electrode Approximation - has been developed to approximate the coordinates of invisible base electrodes, and therefore, to enable superposition on SPECT images and EEG maps in case of incomplete 3D data.

Error of the approximation of the coordinates of the missing electrodes using the developed method is relatively large. The way to increase the accuracy of this method is to prepare the model as highly representative for the population as possible. Nevertheless, this approach is much more accurate than using a standard model, usually spherical, that is applied in the methods for electrode localization in the commercial systems for EEG recordings analysis.

### REFERENCES

- [1] McNally, K.A., Paige, A.L., Varghese, G., Zhang, H., Novotny, E.J., Spencer, S.S., Zupal, G., Blumenfeld, H. (2005). Localizing value of ictal-interictal SPECT analyzed by SPM (ISAS). *Epilepsia*, 46, 1450-1464.
- [2] O'Brien, T.J., So, E.L., Mullan, B.P., Hauser, M.F., Brinkmann, B.H., Bohnen, N.I., Hanson, D., Cascino, G.D., Jack, C.R. Jr, Sharbrough, F.W. (1998). Subtraction ictal SPECT coregistered to MRI improves clinical usefulness of SPECT in localizing the surgical seizure focus. *Neurology*, 50, 445-454.

- [3] Kowalczyk, L., Bajera, A., Goszczynska, H., Zalewska, E., Krolicki, L. (2013). Superposition of 3D EEG maps on SPECT images acquired from simultaneous examinations. *Biocybernetics and Biomedical Engineering*, 33, 196-203.
- [4] Goszczyńska, H., Królicki, L., Bajera, A., Zalewska, E., Kowalczyk, L., Walerjan, P., Rysz, A., Kolebska, K. (2007). The procedure for SPECT and BEAM images adjustment. *Polish Journal of Medical Physics and Engineering*, 13, 115-125.
- [5] Jasper, H.H. (1958). The ten-twenty electrode system of the International Federation. *Electroencephalography and Clinical Neurophysiology*, 10, 371-375.
- [6] Papademetris, X., Jackowski, M., Rajeevan, N., Constable, R.T., Staib, L.H. *BioImageSuite: An integrated medical image analysis suite*. Section of Bioimaging Sciences, Dept. of Diagnostic Radiology, Yale School of Medicine. <http://www.bioimagesuite.org>
- [7] Koessler, L., Cecchin, T., Caspary, O., Benhadid, A., Vespignani, H., Maillard, L. (2011). EEG-MRI co-registration and sensor labeling using a 3D laser scanner. *Annals of Biomedical Engineering*, 39, 983-995.
- [8] Koessler, L., Maillard, L., Benhadid, A., Vignal, J.P., Braun, M., Vespignani, H. (2007). Spatial localisation of EEG electrodes. *Clinical Neurophysiology*, 37, 97-102.
- [9] Oostenveld, R., Praamstra, P. (2001). The five percent electrode system for high-resolution EEG and ERP measurements. *Clinical Neurophysiology*, 112, 713-719.
- [10] Oostenveld, R., Praamstra, P., Stegeman, D.F., van Oosterom, A. (2001). Overlap of attention and movement-related activity in lateralized event-related brain potentials. *Clinical Neurophysiology*, 112, 477-484.
- [11] de Munck, J.C., van Houdt, P.J., Verdaasdonk, R.M., Ossenblok, P.W. (2012). A semi-automatic method to determine electrode positions and labels from gel artifacts in EEG/fMRI-studies. *Neuroimage*, 59, 399-403.
- [12] Rademacher, J., Caviness, V.S. Jr, Steinmetz, H., Galaburda, A.M. (1993). Topographical variation of the human primary cortices: Implications for neuroimaging, brain mapping, and neurobiology. *Cerebral Cortex*, 3 (4), 313-329.
- [13] Scheinost, D., Teisseyre, T.Z., Distasio, M., DeSalvo, M.N., Papademetris, X., Blumenfeld, H. (2010). New open-source ictal SPECT analysis method implemented in BioImage Suite. *Epilepsia*, 51, 703-707.

Received July 31, 2013.  
Accepted April 11, 2014.